INTERNATIONAL ATOMIC ENERGY AGENCY
UNITED NATIONS EDUCATIONAL, SCIENTIFIC AND CULTURAL ORGANIZATION
INTERNATIONAL CENTRE FOR THEORETICAL PHYSICS
I.C.T.P., P.O. BOX 586, 34100 TRIESTE, ITALY, CABLE CENTRATOM TRIESTE

H4-SMR 393/25

SPRING COLLEGE ON PLASMA PHYSICS

15 May - 9 June 1989

STIMULATED SCATTERING OF LARGE AMPLITUDE WAVES IN THE IONOSPHERE: EXPERIMENTAL RESULTS

Bo Thide

Uppsala Division
Swedish Institute of Space Physics
S-755 91
Uppsala
Sweden

Stimulated scattering of large amplitude waves in the ionosphere: experimental results

Bo Thidé
Swedish Institute of Space Physics, Uppsala Division
S-755 91 Uppsala, Sweden

ABSTRACT

A powerful high-frequency radio wave propagating through the ionospheric plasma acts as a pump and excites parametric and other nonlinear processes. These processes can be observed by using diagnostic Thomson scatter radars to probe the pump-enhanced plasma turbulence or by analysing the scattered pump wave directly. Such analyses performed at high and low latitudes (Tromsø, Norway, and Arecibo, Puerto Rico) have shown that the physics is extremely complicated and that old theory cannot satisfactorily explain all results. These experiments can shed new light on nonlinear plasma physics in general but may also provide means for diagnosing the near-Earth plasma and for testing theories of astrophysical plasma processes.

1. INTRODUCTION

Much of the knowledge we have about plasmas has been acquired through different techniques utilising the generation, scattering, refraction and reflection of electromagnetic radiation (X-rays, lasers, microwaves and radio waves) in these media. Such techniques are very attractive since they render possible the study of different processes also in cases when a local measurement *in situ* in the plasma is, for various reasons, not possible. For instance, the "remote sensing" of processes in fusion reactors in the laboratory, or studies of small- or large-scale phenomena in space plasma or in astrophysical systems.

For example, the technique of ionospheric sounding, which consists of transmitting short radio pulses in the high frequency (HF) regime of typically 2–16 MHz and measuring the characteristics of the echoes from the ionosphere, relies on the fact that for small and modest powers the ionospheric plasma responds linearly. This technique has been used successfully for over 50 years and has provided a wealth of information on our near-Earth space environment.

However, it is well known that the dynamics of all plasmas, including the ionosphere, is governed by nonlinear laws and that the linear models commonly used are only approximations to the true plasma behaviour. For instance, the linear dispersion laws often used to describe various wave modes are, even if they are derived in full kinetic (Maxwell-Boltzmann) theory, strictly speaking, valid only for infinitesimally small wave amplitudes. In fact, a particular type of nonlinear interaction between two different radio waves propagating through the same region of the ionosphere was observed already in the 1930's and is since then called the Luxembourg effect.[1]

When installations for intentional modification of the near-Earth plasma by strong radio wave irradiation were being built in the 1970's it was generally believed that the most important effect would be a local heating of the plasma—hence the name "heating" facilities. Soon it became clear that nonlinear wave processes could be excited and observed in these experiments. This was a new way of working in space plasma physics. We were now able to abandon the traditional "morphology" technique where one passively observes those phenomena that Nature creates in an uncontrolled way at unpredictable times, and instead we study the effects of controlled perturbations in a "stimulus/response" fashion as in almost all other physics research work. Because of this difference, ionospheric heating experiments are sometimes said to belong to the class of "active" experiments.

In recent years there has been an intensified activity in the study of nonlinear wave phenomena (parametric instabilities, solitons, cavitons, *etc*). The near-Earth plasma, where parameters like the electron concentration, temperature, collision frequency and so on vary within large intervals, is especially well suited for such basic studies and in itself a region which is rich in natural nonlinear phenomena. Therefore, ionospheric modification experiments are providing a means for testing modern developments in the area of large amplitudes and fields in plasma. At the same time these experiments provide insight into the fundamental processes that govern the dynamics of the natural near-Earth plasma.

The literature describing the progress of studies of nonlinear wave processes in ionospheric modification experiments is abundant.[2–9]

2. THE NEAR-EARTH PLASMA

The ionosphere is the transition region between the non-ionised atmosphere and the fully ionised magnetosphere. Hence, the physical (and chemical) properties of the ionosphere vary significantly with altitude. The degree of ionisation is low, with a ratio of the concentration of charged particles to that of neutral atoms and molecules varying from 10^{-8} to 10^{-4} between 100 and 300 km altitude and reaching about 10^{-1} at 1000 km.

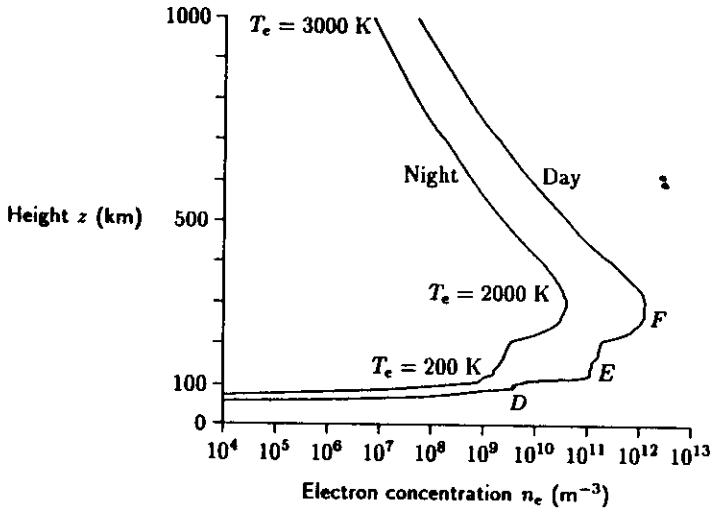

Figure 1. Schematic plot of the electron density profile in the ionosphere for day and night conditions, respectively. The D, E, and F layers of more or less constant electron concentration are depicted. The values of the electron temperature, T_e, varies with height, latitude and time. The ions in the F layer are predominantly O^+ whereas at lower altitudes O_2^+ and NO^+ dominate. Typical ion temperatures are 0.5–1.0 T_e.

The region of the ionosphere where most of the experiments described here have been performed is called the F region, between roughly 150 and 300 km; see Fig. 1. In this region the plasma is a low-β plasma, *i.e.*, the particle pressure to magnetic field pressure ratio is small, of the order 10^{-5}, and the geomagnetic field can be considered unperturbed by the presence of the plasma. Furthermore, the F region plasma is weakly collisional, with the electron mean free path of the order one kilometer. The electron Debye length λ_{De} is of the order one centimetre or less.

3. Experimental facilities

The heating modification facilities used are nothing but very powerful radio transmitters operating in the frequency range of roughly 1–10 MHz, *i.e.*, typical ionospheric plasma frequencies, and beaming its power into the overhead ionosphere via large high-gain antennas.

The following table of ionospheric modification facilities and their main properties is not necessarily correct or complete. It may, however, serve as a list of typical parameters for such installations. Facilities at different latitudes give access to the ionosphere under different geomagnetic and geophysical conditions.

Ionospheric Modification Facilities

Location	*Year*	*Freq* (MHz)	*ERP* (MW)	*Antenna gain/size*	*Modulation*	*Polarisation*
Arecibo, Puerto Rico 18.35°N, 66.75°W	1976	3.1-8.3	60	25 dB	CW, AM, Pulse	O/X
Tromsø, Norway 69.58°N, 19.21°W "Heating"	1981	4.0-8.0	360	24 dB	CW, AM, Pulse	O/X, Linear
Fairbanks, Alaska "HIPAS"	1982	3	40	19 dB	Pulse	O/X
Moscow, USSR 56°N, 37°E	1981	1.35	1000	1000m×1000m	Pulse 500 μs, PRF=50 Hz	O/X
Gorky, USSR 56°N, 44°E "Zimenky" "Sura 1 & 2"	1972, 1980	1.2-1.5 2.5-3.0 3.3-5.8 4.5-9.3	5 2 20 300	500m×300m 150m×70m 150m×200m 300m×300m	CW, Pulse 100 μs	O/X
Dyushanbe, USSR 35°N, 59°E	1983	4-6	9	150m×150m	CW	O/X
Kharkow, USSR 50°N, 36°E	1986	5	20	150m×150m	Pulse 2.8 ms, PRF=100 Hz	O/X
Murmansk, USSR 68°N, 33°E	1976	3.3	10	400m×400m	CW	Linear

At two of the most important modification facilities, Arecibo, Puerto Rico, and Tromsø, Norway, incoherent scatter radars are available (Arecibo 430 MHz, EISCAT 933 and 224 MHz). These radars can be used to probe the ionosphere for longitudinal, electrostatic waves and the technique can be described crudely as follows:

When the frequency of the incident radar beam, ω_{inc}, is much higher than the plasma frequency, ω_p, most of the radar beam energy propagates straight through the plasma. However, each electron in the plasma has a very minute scattering cross section and gives rise to Thomson scattering of the incident RF wave. When the electrons move collectively, as they do when they oscillate in a longitudinal wave, the extremely weak scattering from each individual electron adds up incoherently in a Bragg-like fashion to a larger, but still weak, scattering which is enough to be observed by powerful and sensitive radars. The scattered signal will be Doppler shifted due to the motion of the target. Since the target in this scattering process are the phase planes in a longitudinal wave which move at the wave phase velocity, and the phase velocity is proportional to the wave frequency, the measured Doppler shift in the scattered signal gives information on the frequency of the longitudinal wave. Because of the Bragg condition constraint, which requires that the scattering wave has a wavelength equal to half that of the radar (constructive interference), a single radar can measure the frequency of electrostatic waves at the two wave vectors $\pm 2\mathbf{k}_{inc}$ only. Approaching waves give rise to a positive Doppler shift and receding waves to a negative one.

Longitudinal electron plasma (Langmuir) waves $(\omega_e, \mathbf{k}_e)$ propagating in a weakly inhomogeneous plasma at an angle θ_e to the terrestrial magnetic field $\mathbf{B}_T$ fulfil the generalized dispersion law, valid under the assumption of $\sin^2\theta_e\,\omega_{ce}^2/\omega_p^2 \ll 1$,

$$\omega_e = \omega_p \left(1 + 3\frac{k_e^2}{k_{De}^2} + \frac{\omega_{ce}^2}{\omega_p^2}\sin^2\theta_e\right)^{1/2} \tag{1}$$

where $k_{De} = 1/\lambda_{De}$ and $\omega_{ce} = |eB_T|/m_e$ is the electron cyclotron frequency. Solving for the wave number, we can rewrite this as

$$k_e^2(z) \approx \frac{1}{3}\frac{\omega_e^2}{v_e^2}\left(1 - \frac{\omega_p^2(z) + \omega_{ce}^2\sin^2\theta_e}{\omega_e^2}\right) \tag{2}$$

Here, $v_e = \sqrt{\kappa T_e/m_e}$ is the thermal velocity of the electrons; κ is Boltzmann's constant and T_e and m_e are the electron temperature and mass, respectively. Scattering off these waves will produce two lines, at $\omega_{inc} \pm \omega_e$. These signatures in the incoherent scatter spectrum are called plasma lines.

Likewise, longitudinal electrostatic ion waves $(\omega_i, \mathbf{k}_i)$, which have very low frequencies, will give rise to ion lines at $\omega_{inc} \pm \omega_i$. For not too large or small k_i values, we assume this wave to be an ion acoustic mode:

$$\omega_i \approx \omega_{ia} = c_a k_i = a\sqrt{\frac{m_e}{m_i}}v_e k_i \tag{3}$$

In the ionosphere, with its typical ion to electron temperature ratio $T_i/T_e \lesssim 1$, the function a can be approximated by

$$a = \frac{1}{\sqrt{2}}(1+\delta)\left(1 + \sqrt{1 + 12\frac{T_i}{T_e}}\right)^{1/2} \tag{4}$$

where δ is a small parameter which, in typical ionospheric modification experiments, is about 0.13. That this is a convenient parametrization can be seen by comparing with numerical solutions. For $\delta = 0$ one recovers the analytic approximation for the linear, small k_i dispersion law, derived by using kinetic theory and standard expansions of the plasma dispersion function. Furthermore, if $T_i/T_e \ll 1/12$, which is normally not the case in ionospheric modification experiments, one obtains $a \approx (1 + 3T_i/T_e)^{1/2}$, a crude approximation often used.

It is important to bear in mind that, according to Eq. (1), ω_e is directly proportional to ω_p which is a varying function with altitude (see Fig. 1) and the plasma lines observed in ionospheric experiments will therefore be smeared out to contain frequency components (with a certain weighting factor) corresponding to different plasma frequencies within the volume illuminated by the finite-width radar pulse. This is not the case for the ion lines; *cf.* Eq. (3).

As we shall see later, a powerful HF radio wave can enhance the plasma turbulence and hence give rise to strong plasma and ion lines. The incoherent scatter radar technique has therefore become a very important tool for studying various nonlinear phenomena involving longitudinal waves. Of course, these enhanced waves can propagate only within the ionospheric plasma and, since they are often heavily damped, are very localised.

Transverse electromagnetic waves, on the other hand, can propagate long distances, carrying with them information from the source region and the medium they propagate through. It is therefore interesting to know that in addition to the the longitudinal waves observable with scatter radars, secondary EM radiation is produced in the ionospheric modification experiments. This phenomenon, which was discovered in 1981 in Tromsø,[10] is now known as stimulated electromagnetic emission (SEE). Results obtained with the SEE technique will be the emphasis of this treatment.

4. The pump wave

All the effects that are observed in the ionospheric modification experiments are, of course, caused by the interaction of the strong EM modifier wave and the ionospheric plasma, including any waves that are present in it. In order to interpret these effects it is essential to be able to describe this EM wave in detail. Often, it is advantageous to have accurate analytical expressions for this wave even if these expressions are valid only under certain simplifying assumptions.

General analytical formulas for the field distribution of a vertically propagating electromagnetic wave, neglecting nonlinear effects, have been derived by *Lundborg and Thidé*.[11,12] These formulas are derived within a uniform approximation, valid throughout the reflection region, and do not break down close to the reflection point as in the WKB approximation.

The linear propagation of an electromagnetic wave is described by the wave equation, which is obtained from Maxwell's equations. Describing the ionosphere as a cold plasma with infinitely heavy ions and the electron concentration gradient in the vertical direction, which is a very good model in our case, the wave equation for the E field of the vertically propagating radio wave can be written in component form as follows:

$$\frac{\partial^2 E_x}{\partial z^2} + k_v^2 Q_{xx}(z) E_x + k_v^2 Q_{xy}(z) E_y = 0 \tag{5}$$

$$\frac{\partial^2 E_y}{\partial z^2} + k_v^2 Q_{yx}(z) E_x + k_v^2 Q_{yy}(z) E_y = 0 \tag{6}$$

$$E_z + Q_{zx}(z) E_x + Q_{zy}(z) E_y = 0 \tag{7}$$

The subscripts x, y, and z, denote the magnetic east, magnetic north, and vertical components, respectively. The vacuum wave number is given by $k_v = \omega_0/c$, where c is the speed of light.

Notice that nonlinear terms have been neglected. Even if we are after nonlinear effects, the pump field strength in our experiments is still small enough so that the linear wave equations are good approximations, at least initially before turbulence sets in. They are therefore a good starting point in a theoretical analysis.

As we see, the wave equations are coupled and the coupling coefficients depend on the spatial variable z.

The solution for the ordinary mode electric field vector at an arbitrary point z can be written[13]

$$E_x(z) = \rho(z) F_O(z) \tag{8}$$

$$E_y(z) = F_O(z) \tag{9}$$

$$E_z(z) = \rho(z) \rho_L(z) F_O(z) \tag{10}$$

where

$$\rho = i \frac{\omega_{ce}^2 \sin^2\theta - \left[\omega_{ce}^4 \sin^4\theta + 4\left(\omega_0^2 + i\nu\omega_0 - \omega_p^2\right)^2 \frac{\omega_{ce}^2}{\omega_0^2} \cos^2\theta\right]^{1/2}}{2\left(\omega_0^2 + i\nu\omega_0 - \omega_p^2\right) \frac{\omega_{ce}}{\omega_0} \cos\theta} \tag{11}$$

$$\rho_L = \frac{i\omega_0 \omega_{ce} \sin\theta}{\omega_0^2 + i\nu\omega_0 - \omega_p^2} \left(n_O^2 - 1\right) \tag{12}$$

and ω_0, ν, ω_{ce}, ω_p, and n_O denote the wave angular frequency, effective electron collision frequency, cyclotron angular frequency, plasma angular frequency, and ordinary mode refractive index, respectively. The geomagnetic field is taken to be in the yz-plane.

For the case of a monotonically increasing electron concentration with height the refractive index has one simple zero ($z = z_0$) and the function F_O in the uniform approximation is given by

$$F_O(z) = \frac{A}{(\rho^2 - 1)^{1/2}} \left[\frac{-\Phi(z)}{k_v^2 n_O^2(z)}\right]^{1/4} \mathrm{Ai}(\Phi(z)) \tag{13}$$

where A is a constant related to the field amplitude below the ionosphere, Ai is one of the

Airy functions, and

$$\Phi = \left(-i\frac{3}{2}\zeta\right)^{2/3} \tag{14}$$

$$\zeta = k_v \int_{z_0}^{z} n_O(z)\, dz \tag{15}$$

For a linear concentration profile of scale height H the plasma frequency as a function of altitude z is given by

$$\omega_p^2 = \omega_0^2 \left(1 - \frac{z_0 - z}{H}\right) \tag{16}$$

where ω_0 is the plasma frequency at the reflection height z_0. In the case of an ordinary mode pump wave which is vertically incident on the ionosphere the plasma frequency at the reflection height equals the pump frequency. The linear profile is a reasonable approximation of a sufficiently small region at the reflection height for any smoothly varying overdense ionospheric electron concentration profile. With

$$z_0 - z \ll H \tan^2\theta \tag{17}$$

the refractive index in the so called quasi-transverse (QT) approximation[14] adopted here is expressed as

$$n_O(z) \approx \left(\frac{z_0 - z}{H \sin^2\theta}\right)^{1/2} \left(1 - \frac{z_0 - z}{2H \tan^2\theta}\right) \tag{18}$$

where we only kept the first two terms in the series expansion. Integrating from the height of reflection z_0, down to z, yields

$$\int_{z_0}^{z} n_O(z)\, dz \approx -\frac{2}{3} \frac{(z_0 - z)^{3/2}}{(H \sin^2\theta)^{1/2}} \left[1 - \frac{3}{10} \frac{(z_0 - z)}{H \tan^2\theta}\right] \tag{19}$$

With this result in (15) we have an analytic formula for the ordinary mode electric field strength in the QT approximation of the refractive index, for the case of a linear electron concentration profile.

The positions of the successive standing wave maxima are approximately given by the maxima of the Airy function in (13). Equation (14) for the argument of the Airy function gives

$$(z_0 - z)\left[1 - \frac{3(z_0 - z)}{10H \tan^2\theta}\right]^{2/3} \approx -\Phi \left(\frac{H \sin^2\theta}{k_v^2}\right)^{1/3} \tag{20}$$

Solving this equation for $z_0 - z$ by the method of successive approximation gives for the distance between the reflection height and the nth wave maximum

$$z_0 - z_n \approx -\Phi_n \left(\frac{H \sin^2\theta}{k_v^2}\right)^{1/3} \left[1 - \frac{\Phi_n}{5H \tan^2\theta} \left(\frac{H \sin^2\theta}{k_v^2}\right)^{1/3}\right] \tag{21}$$

where Φ_n is the argument of the Airy function at its nth maximum ($\Phi_1 \approx -1.019$, $\Phi_2 \approx -3.248$, $\Phi_3 \approx -4.820$, $\Phi_4 \approx -6.163$).[15] Equation (21) is a more accurate formula than the version given by *Gurevich*[16] who only included the first term on the right-hand side. It is

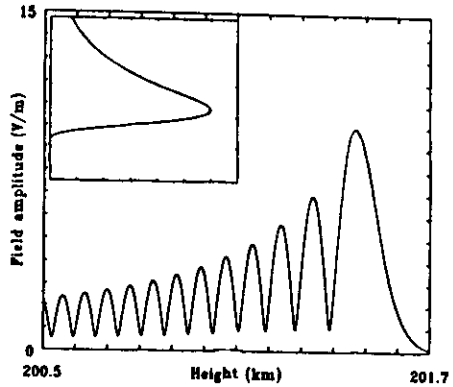

Figure 2. Electric field strength $|\mathbf{E}_0|$ in V/m for an upgoing O mode radio wave, normalised to 1 V/m at $z = 100$ km, as a function of altitude near the reflection point ($z = 201.525$ km). The wave frequency of 5.423 MHz is chosen to be below the plasma frequency at the maximum of the Chapman profile used (critical frequency). The profile is depicted in the inset (horisontal scale: plasma frequency 0–7000 kHz, vertical scale: height 0–500 km). The geomagnetic field makes an angle of 12.8° to the downward vertical and the electron cyclotron frequency is 1.350 MHz, corresponding to the geophysical situation at Tromsø. After *Thidé and Lundborg*.[13]

apparent that the electric field distribution in the ionospheric reflection region is strongly dependent on the geomagnetic field angle.

In Figure 2, a realistic Chapman profile with an exponentially varying collision frequency[14] was chosen as the ionospheric model and the standing wave pattern (absolute value of the electric field amplitude) was calculated.

To summarize, the electric field strength is maximum just below the reflection height of the pump wave. Swelling is strongest in the case of a small magnetic field angle and a short electron concentration scale height. It is therefore likely that the reflection region is the source of a number of plasma processes, such as nonlinear wave interactions, cavity formation, and particle acceleration. It is also likely that nonlinear plasma phenomena requiring high electric field strengths will be more easily excited near the geomagnetic poles than at lower latitudes.

5. Parametric signatures

As was shown in Section 4, the electric field of the radio waves produced at the ionospheric modification facilities is very strong. One can therefore expect nonlinear effects to arise when these waves propagate in the near-Earth plasma. Particularly, near the altitude in the ionosphere where the waves are normally reflected, very strong standing waves are set up. The nonlinear effects of interest to us are mainly those that result in the transfer of energy from one mode to another. These pump-enhanced modes, which are normally absent or too weak to be observed, contain a lot of information and are often easy to study experimentally using modern signal analysis.

As is well known, the self-consistent theory of nonlinear wave interactions in plasmas is extremely complicated. However, working in the weak turbulence regime, *i.e.*, considering

the weak interaction between a strong pump ("mother") and weak, linear daughter modes and neglecting nonlinear effects as saturation and pump depletion, one can describe these interactions in fairly simple terms; they are called parametric instabilities. In this section, we shall consider the kinematics of such instabilities in the simplest of cases and formulate a few quantitative rules of thumb that we can use to analyse the experimental results. We shall see later that a number of the phenomena we observe can be explained surprisingly well in terms of parametric processes, but we shall also see that this simple theory is incapable of explaining certain prominent features in the experimentally observed spectra. The general theory of parametric instabilities in plasmas was derived in the 1960's[17–20] and later applied to the ionosphere.[21,22]

From the dispersion law (1) we see that the influence of an external magnetic field on Langmuir waves is negligible if they propagate nearly parallel or antiparallel to this field. This is the case in many of the ionospheric heating experiments. Let us therefore, for simplicity, assume that we can neglect the effect of the geomagnetic field on the parametric processes altogether. That means that we consider only transverse EM waves, electron plasma (Langmuir) waves, and ion acoustic waves and their interactions. In quantum parlance we can describe this as the interaction between, and creation and annihilation of, photons, plasmons, and phonons, respectively. Furthermore, we limit ourselves here to the interaction between three waves/quanta.

The conservation of energy and linear momentum in such a process can be written:

$$\hbar\omega_{\text{mother}} = \hbar\omega_{\text{daughter}_1} + \hbar\omega_{\text{daughter}_2} \tag{22}$$

$$\hbar\mathbf{k}_{\text{mother}} = \hbar\mathbf{k}_{\text{daughter}_1} + \hbar\mathbf{k}_{\text{daughter}_2} \tag{23}$$

and can be described diagrammatically as in Figs. 3–7. Cancelling $\hbar$ in the conservation laws above, we obtain matching conditions for the frequencies and wave vectors of the waves. In the parametric processes we describe below, these matching conditions are assumed to be (approximately) fulfilled.

5.1 Parametric Decay Instability (PDI)

In the PDI process the transverse EM pump, $(\omega_0, \mathbf{k}_0)$, decays into an ion acoustic mode $(\omega_i, \mathbf{k}_i)$ and an electron plasma (Langmuir) mode $(\omega_e, \mathbf{k}_e)$ and the matching conditions can be written

$$\omega_e = \omega_0 - \omega_i \tag{24}$$

$$\mathbf{k}_e = \mathbf{k}_0 - \mathbf{k}_i \approx -\mathbf{k}_i \tag{25}$$

where the last approximation is valid because $k_0 \approx k_e v_e/c \ll k_e$; this is often called the dipole approximation.

Inserting these matching conditions into the linear dispersion laws for the participating modes, one finds, to lowest approximation order, that the strongest PDI excitation will occur for

$$k_e \approx \sqrt{\frac{m_e}{3\kappa T_e}}\left(1 - \frac{\omega_p}{\omega_0}\right)^{1/2} \tag{26}$$

In Fig. 3 we illustrate how a 1-dimensional PDI process and its characteristics can be

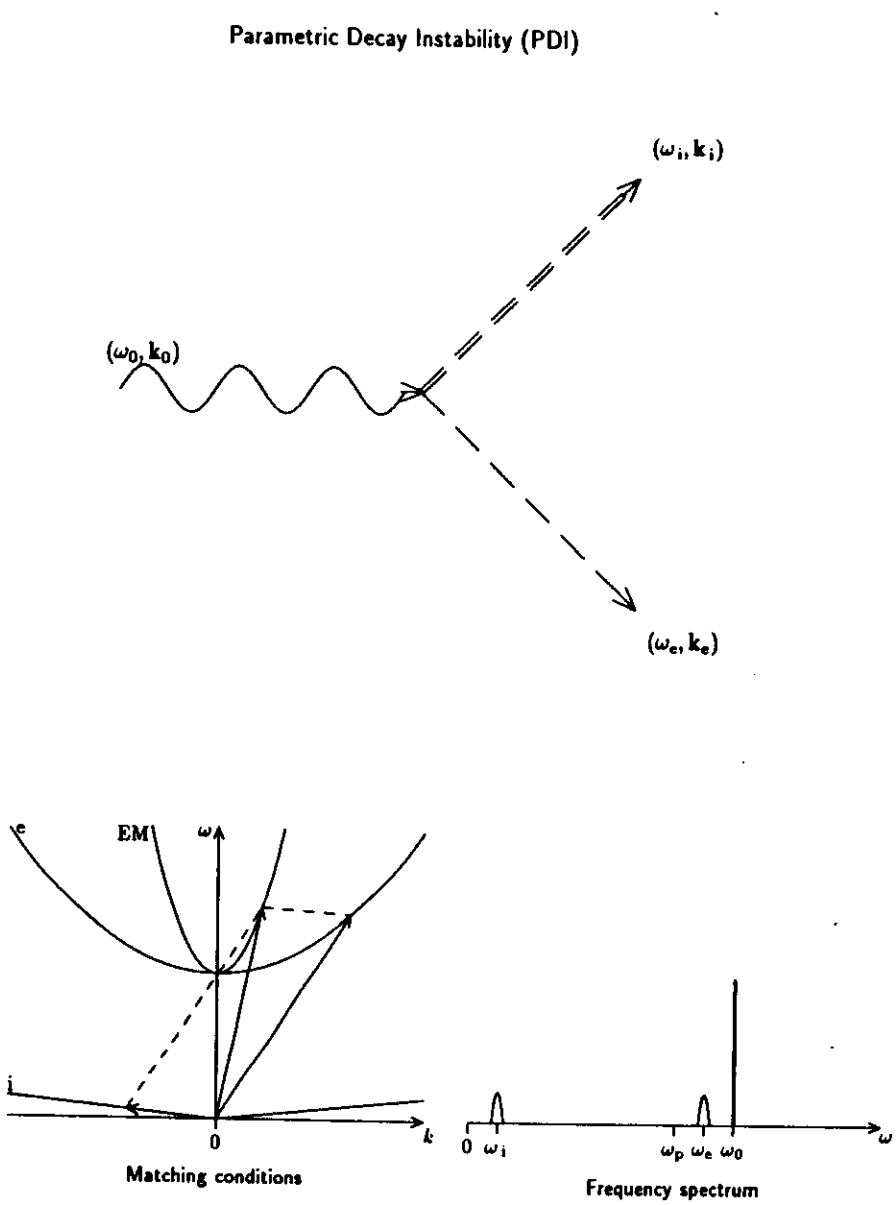

Figure 3. The decay of a photon into a phonon and a plasmon.

described schematically. The top diagram describes the decay itself, the bottom left hand diagram describes the simultaneous fulfillment of the matching conditions and dispersion laws, and the bottom right diagram depicts the spectrum of waves we can expect for the given wave vectors.

In the ionosphere the plasma frequency varies with height z, and $k_e \approx k_i$ for the strongest PDI is therefore dependent on z. If the profile is monotonically increasing with z, the PDI daughter waves will have a larger wave number further down the profile until the wave number becomes so large that strong Landau damping prohibits the process. Hence, there is a region immediately below the reflection point where PDI can be excited and where, at the point of excitation, each altitude corresponds to a unique (narrow range of) k_i. Now, using Eq. (3) we can calculate the ion acoustic frequency and, since ω_0 is fixed in the experiment, also the Langmuir frequency for each altitude. It turns out that the spectrum of Langmuir waves is asymmetric ranging from the pump frequency to a few 10 kHz below it.

The threshold field strength, *i.e.*, the magnitude of $\mathbf{E}_0$ which has to be exceeded for the PDI to be excited in the ionosphere, is of the order 0.2 V/m. This is much lower than the field strength of the waves from ionospheric modifiers when operated at full power. There is therefore reason to believe that the simple theory discussed here is only applicable, if at all, when the HF transmitter level is kept low or in the regions outside the main lobe of the transmitter antenna.

5.2 Electron Decay Instability (EDI)

This process, in which a Langmuir wave decays into another Langmuir wave and an ion acoustic wave, is illustrated in Fig. 4. It is an important process in ionospheric modification experiments since a Langmuir daughter in a PDI can act as a mother in an EDI and cascade energy away down to lower k. However, for $k_e/k_{De} < a(m_e/m_i)^{1/2}/3$, where a is given by Eq. (4), further decays are kinematically forbidden and we may face the problem of plasmon condensation.[23] The finite number of EDI cascades will give rise to ion acoustic and Langmuir pairs with successively smaller k and lower frequency. This means that the total Langmuir spectrum will be broader at the low frequency end and may range down to 50–100 kHz below the pump frequency.

5.3 Stimulated Brillouin Scattering (SBS)

The SBS is different from PDI and EDI inasmuch as one of the daughter modes is a transverse EM wave which may propagate out of the plasma. In the backscattering geometry, the SBS ion daughter mode has a $k_i \approx 2k_0$ and is therefore very small. In the ionosphere this corresponds to a negative frequency shift of the EM daughter of a few tens of Hz. The SBS process is illustrated in Fig. 5. However, the convective SBS may be difficult to excite unless the plasma density is fairly constant as a function of z.

5.4 Stimulated Raman Scattering (SRS)

Like the SBS, the SRS also has an EM daughter. But, since the other daughter is a Langmuir wave, the SRS is only excited for $\omega_o \geq 2\omega_p$ since otherwise the daughters would be evanescent. Hence, this process can only occur in the ionosphere at or below the quarter-critical point(s). The convective losses for SRS in the ionosphere are thought to be severe. See Fig. 6.

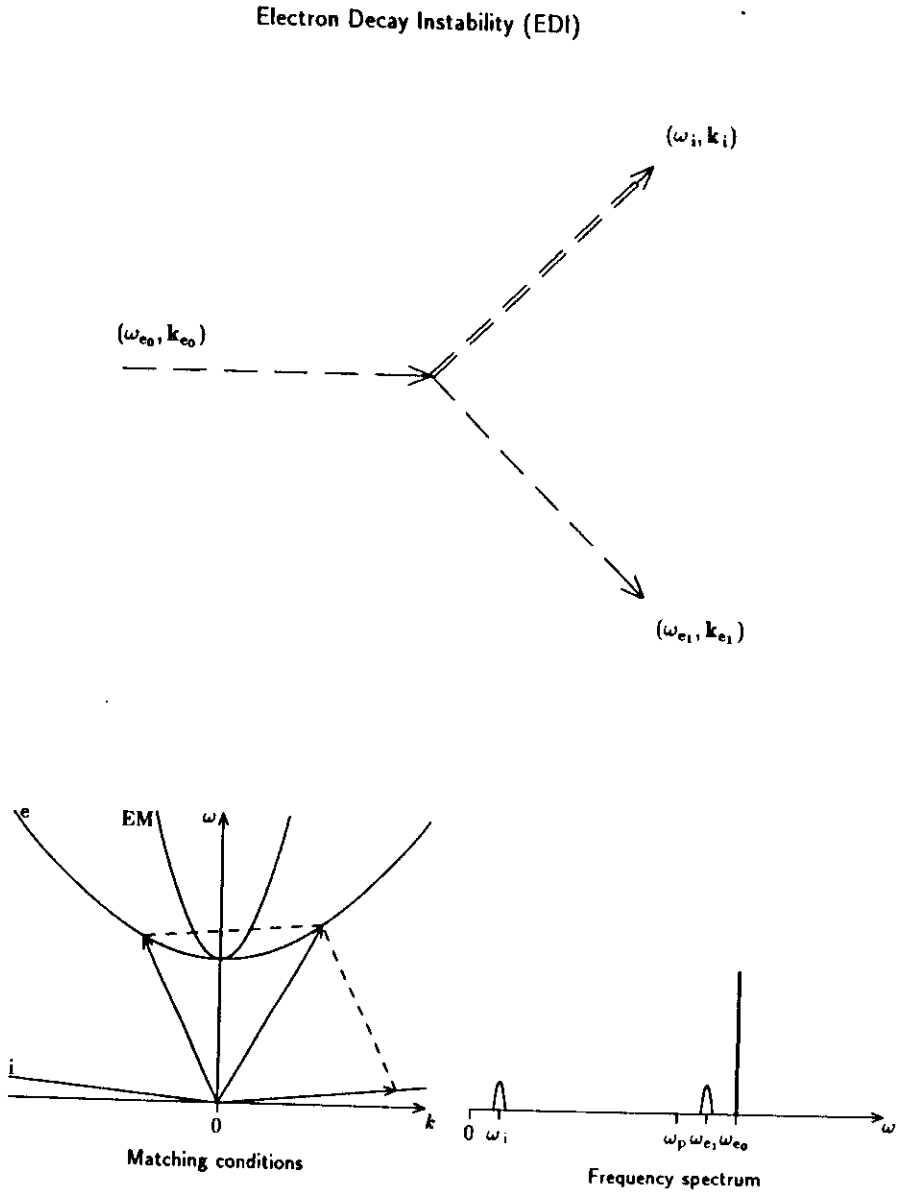

Figure 4. The decay of a plasmon into a phonon and a plasmon.

Stimulated Brillouin Scattering (SBS)

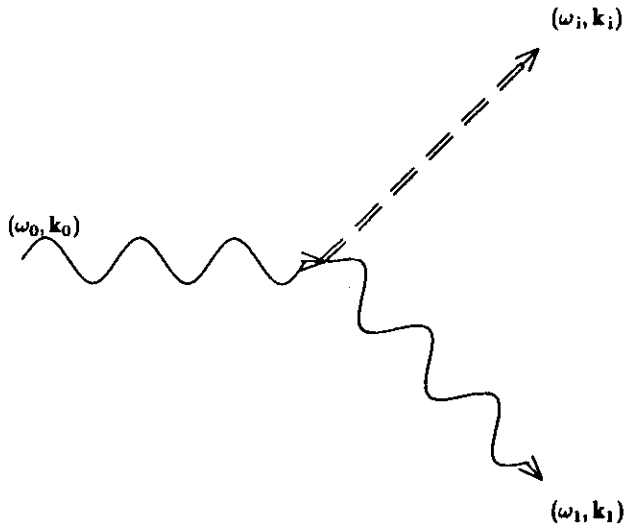

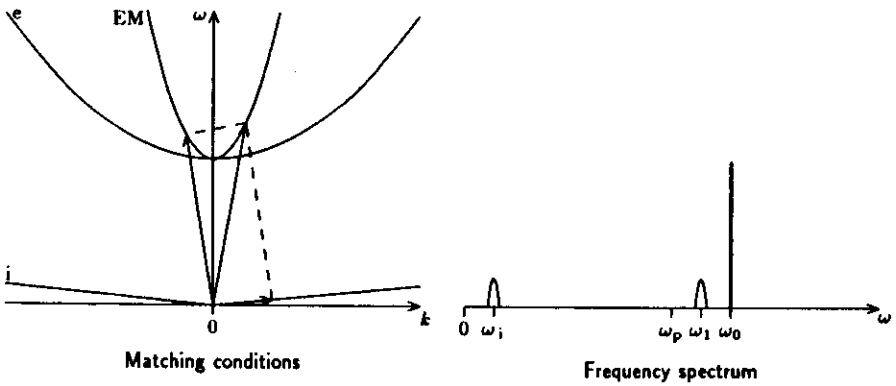

Figure 5. The decay of a photon into a phonon and a photon.

Stimulated Raman Scattering (SRS)

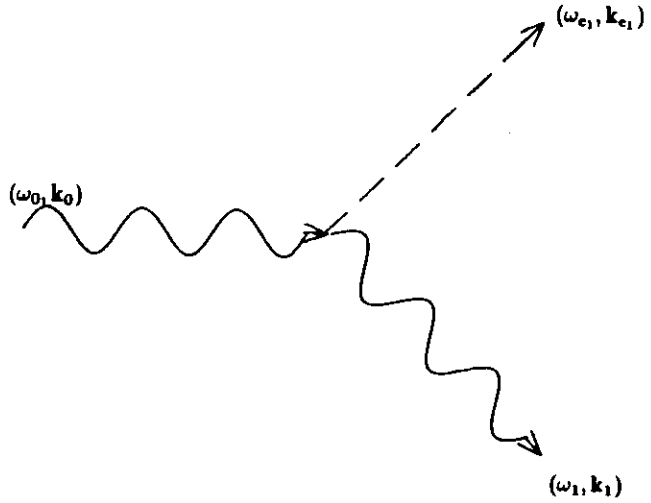

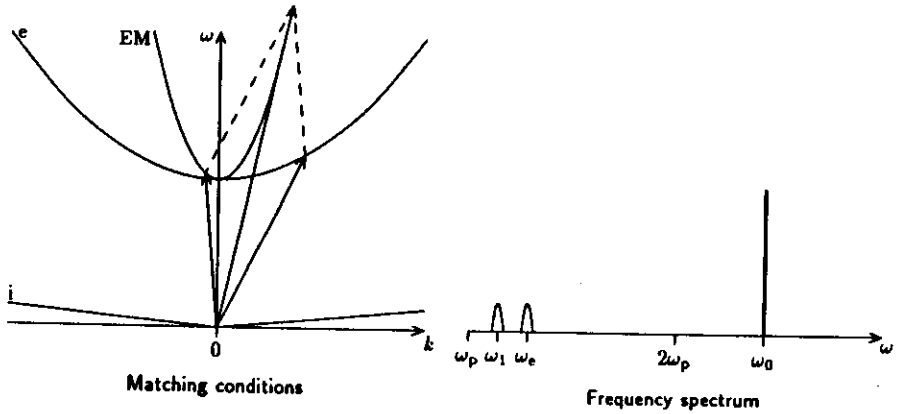

Figure 6. The decay of a photon into a plasmon and a photon.

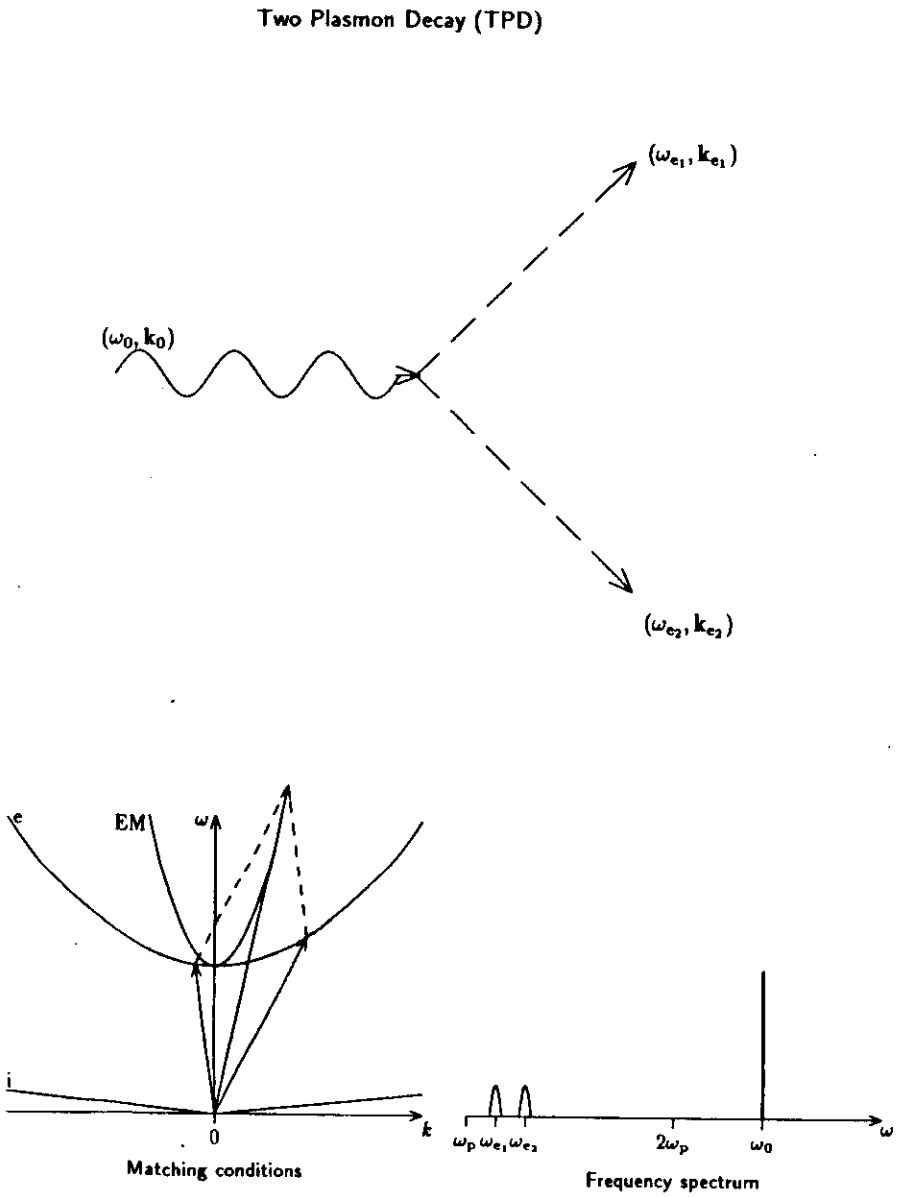

Figure 7. The decay of a photon into two plasmons.

5.5 Two Plasmon Decay (TPD)

The TPD is a process where both daughters are Langmuir waves. Again the mother must have a frequency of at least twice the plasma frequency for this process to occur. The convective damping of the TPD process, and a corresponding threshold, is high in the ionosphere, but often not as high as for the SRS. The TPD process is illustrated in Fig. 7.

6. Experiments

6.1 Incoherent scatter radar

The first ionospheric HF modification experiments were carried out at Platteville, Colorado, USA. One of the important discoveries made in these experiments was that strong HF irradiation can cause the formation of electron density irregularities elongated in the direction of the geomagnetic field. These irregularities, known as field-aligned striations, give rise to backscattering of HF and VHF radar beams intersecting the irregularities at right angles to the magnetic field; for an excellent account on the Platteville results, see the special 1974, Volume 9, Number 11 issue of *Radio Science*.

Since the very first experimental identification in 1971 at Arecibo of the parametric decay of the heater wave into electron and ion plasma waves,[24,25] there has been rapid development within this area of space plasma physics. In particular, with the advent of the MPAe Heating Facility in Tromsø around 1980, new and unique opportunities for studies of nonlinear wave interactions were opened up. Not only was it possible to repeat earlier experiments under vastly different conditions but novel diagnostic techniques were developed and a number of new and surprising observations were made.

The pioneering discoveries at Arecibo were done by spectrum analysing the incoherent scatter radar return from the ionospheric F layer in the presence of a strong HF radio wave $(\omega_0, \mathbf{k}_0)$. Strongly enhanced spectral features were seen and their frequencies, for the incident wave vector $\mathbf{k}_{\rm inc}$ of the 430 MHz radar used, matched those expected to arise from a PDI, namely ion lines at $\omega_{\rm inc} \pm \omega_i(2k_{\rm inc})$ and plasma lines at $\omega_{\rm inc} \pm (\omega_0 - \omega_i(2k_{\rm inc}))$; see the "enhanced ion line" and "decay mode" features in Fig. 8.

Since then, a huge number of HF modification events have been studied at Arecibo with an ever increasing degree of resolution and sensitivity. In most of these experiments the incoherent scatter radar has been the main diagnostic instrument. While it is impossible to present all the interesting discoveries here, one can say that many of the signatures observed agree with predictions from weak turbulence. However, others cannot be explained with this theory. That is true, for instance, for the discoveries made with a new "chirp" radar diagnostic technique which seem to be evidence of the creation of small scale cavitons near the point of pump reflection.[27]

Heating experiments at Tromsø, where the European Incoherent Scatter (EISCAT) radar has been used as a diagnostic, have shown that for very short radar wavelengths (UHF) the results are quite erratic whereas the features seen with the longer wavelength VHF radar are more reproducible and, at least in certain respects, resemble those obtained at Arecibo. Examples of EISCAT UHF spectra of HF enhanced plasma lines are shown in Fig. 9 where strongly developed cascades, similar to those expected from a combined PDI and EDI, can be seen.

In fact, assuming PDI/EDI cascading to be an essentially correct description of the physics, it has been shown how the precise measurement of the position of these cascade lines can provide very reasonable values of the electron number density, electron tempera-

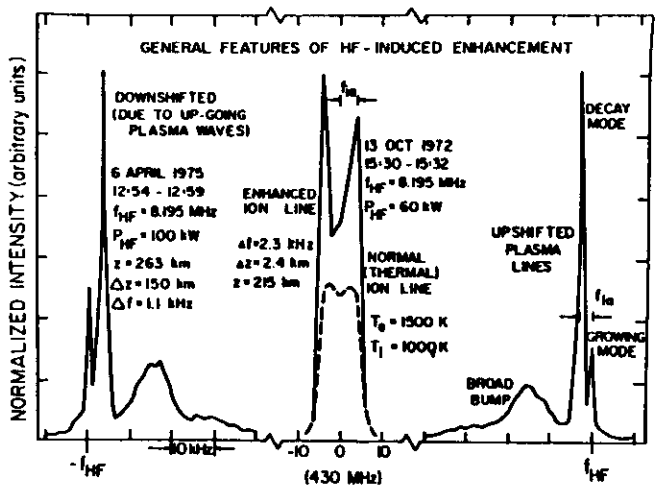

Figure 8. Illustration of typical spectral features in the backscattered radar signal during ionospheric modification experiments. Note the breaks in the frequency scale. The center of the spectrum corresponds to the transmitted radar frequency (430 MHz) and represents radar return with zero Doppler shift. After *Showen and Kim*.[26]

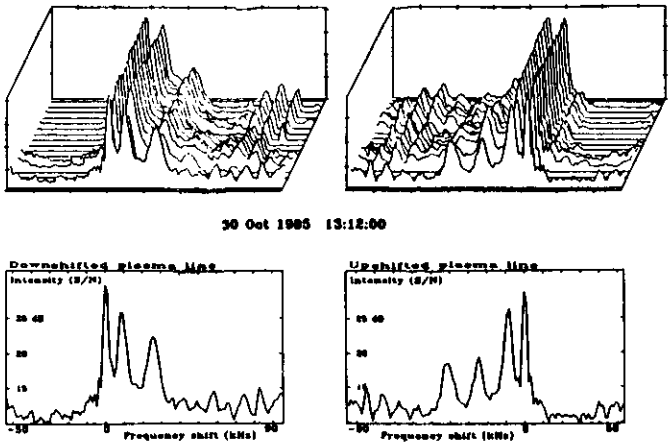

Figure 9. Illustration of HF enhanced cascade-type plasma lines observed 1985 with EISCAT 933 MHz during ionospheric modification experiments. Note the "extra" cascades far out in the spectra. The time resolution was 2 seconds. After *Nordling et al.*[28]

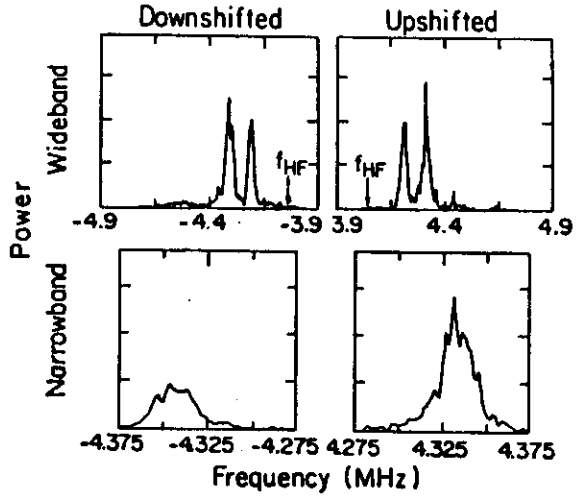

Figure 10. Examples of "displaced" plasma lines observed with EISCAT UHF. According to parametric instability theory, the HF-enhanced plasma lines should appear near the HF frequency (4.04 MHz; marked "f_{HF}"). After *Isham et al.*[30]

ture, and ion temperature during HF modification experiments.[29]

In an attempt to repeat the Arecibo "chirp" experiment mentioned above in the search for caviton signatures under different conditions, a similar experiment was conducted in Tromsø in 1986. No such signatures were found in the EISCAT UHF spectra. Instead one, and sometimes several, new spectral features displaced by a frequency *larger* than the HF heater frequency by a few hundred kHz were consistently observed throughout most of the observing period. Examples of such "displaced" spectra are presented in Fig. 10. Such spectra cannot be predicted by weak turbulence theory.

Inserting the plasma frequency at the reflection height into the dispersion law (1) one finds that for the radar matched k_e this formula gives a Langmuir frequency *upshifted* from ω_0 by approximately 350 kHz. This could indicate that there is a strong excitation of "free" Langmuir modes near the point of HF reflection. Such modes have been found in computer simulations based on strong turbulence theory.[31]

6.1 Stimulated electromagnetic emission

The stimulated electromagnetic emission (SEE) diagnostic technique amounts to monitoring directly the frequency shifted secondary EM radiation that is induced by the strong HF wave in the ionosphere. By using a receiving antenna connected to sensitive and highly accurate HF receivers and spectrum analysers tuned to frequencies near the heater frequency, these emissions can be analysed with respect to amplitude, phase, spectral content and temporal development. This technique was introduced in 1981 in Tromsø[10] and has later been used in Arecibo[32] and the USSR.[9] The SEE technique is complementary to the incoherent scatter technique in the sense that it does not suffer from any Bragg condition constraints and it detects *electromagnetic* radiation generated from all possible plasma wave k vectors.

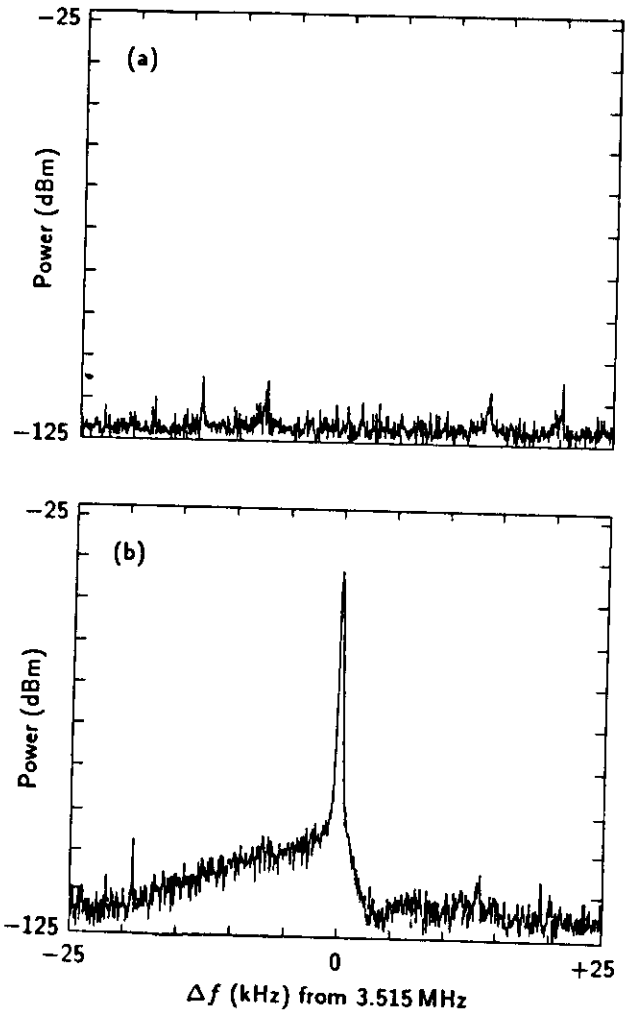

Figure 11. SEE spectra recorded near Tromsø. The top panel (a) shows the background noise spectrum before the pump was turned on. The bottom panel (b) shows the SEE components predominantly in the lower sideband of the ionospherically reflected pump wave at 3.515 MHz (narrow central peak). After *Leyser*.[34]

Fig. 11 displays two spectra recorded in the Lavangsdalen valley, 17 km SSW of the Tromsø heating facility. The top panel (a) was recorded when the HF modifier was off the air and the bottom panel (b) when it was on, beaming its effective radiated power (ERP) of about 280 MW vertically into the overhead ionosphere. The HF wave transmitted on 3.515 MHz is extremely monochromatic (width 1 Hz or less) but the sky radiation measured contains, in addition to the narrow reflected HF wave, frequency components that are downshifted by as much as 25 kHz. The asymmetry of the spectrum is a clear parametric signature but its width excludes the possibility of the SBS process and seems more be what is expected from the PDI. Since PDI generates *electrostatic* modes that cannot be observed directly in the SEE experiments, the process must be a different, possibly more complicated, one. It has been suggested that the broad, skewed SEE spectrum is the result of a PDI process combined with a process that can convert the electrostatic turbulence into escaping EM radiation.[10,33] The efficiency of this conversion seems to be related to the level of striation irregularities.

Often the SEE spectra exhibit a distinct, systematic peak structure. A very common one is the asymmetric intensity maximum, downshifted from the pump frequency ω_0 by approximately $2 \times 10^{-3}\omega_0$. This feature has been observed in SEE experiments in Tromsø and Arecibo; see Fig. 12. The steep edge at the upper frequency end of this feature can possibly be attributed to a parametric decay of upper hybrid waves into lower hybrid waves and downshifted O mode EM radiation. The position of the steep edge corresponds nicely to the frequency of lower hybrid waves propagating near the upper hybrid layer and even scales correctly with the geomagnetic field strength which is different at Tromsø and Arecibo.

In Fig. 13, another systematic feature can be observed. The position of this is of the order 1–2 kHz relative to ω_0 and can be explained in terms of an enhanced PDI level at the first few standing wave maxima of the pump; recall the discussion of the pump wave pattern in Sec. 4. Taking the pump-induced plasma depletion into account and assuming a linear conversion of PDI Langmuir daughter waves into EM waves at these pump maxima, the calculated position of this feature agrees excellently with the experimental values.[35] It may even be possible to estimate the local pump field strength from this position, provided the ionospheric scale length and constituent temperatures are known.

For pump frequencies ω_0 near the harmonics of the ionospheric electron cylotron frequency, ω_{ce}, the Tromsø SEE spectra often exhibit a very pronounced and unique peak structure. Examples of this are presented in Figs. 14 (a)–(c) which were obtained by varying the pump frequency in small steps (20 kHz) around the fourth cyclotron harmonic (≈ 5.4 MHz). In panels (a) and (c) the same lower-hybrid feature as was displayed in Fig. 12 can be observed. This feature is absent in panel (b). What is more striking is the presence of a large, *upshifted* feature in the SEE spectra (a) and (b). The empirical relation for the frequency of the peak of this feature, ω_1, has been established as $\omega_1 \approx 2\omega_0 - n\omega_{ce}$, where n is 3, 4, or 5. This suggests that this is an example of a higher order process involving two pump photons. Clearly, this observation is not explicable in terms of a three-wave parametric instability.

On some rare occasions HF emissions may be generated at $\omega_0/2$. Even though this is expected from an SRS process, the theoretical values of the thresholds, due to plasma inhomogeneities, are predicted to be much higher than the accessible pump field strength. The spectrum displayed in Fig. 15 can therefore only be explained in parametric theory as an absolute SRS occurring at the quarter critical region with a very large local scale

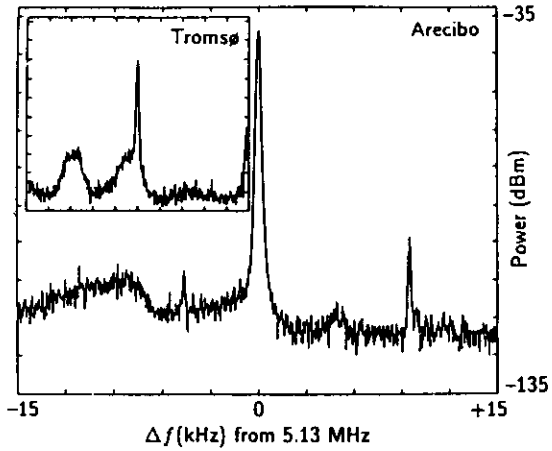

Figure 12. Sky wave power vs. frequency offset Δf from the HF heater frequency 5.13 MHz (60 MW ERP, *O* mode polarization) at Arecibo. The broad maximum at roughly −7 to −15 kHz is due to stimulated electromagnetic emission (SEE) induced in the ionosphere by the heater wave. So is also the weaker feature at about +5 kHz. The very narrow peaks at −5 and +10 kHz are interference from nearby HF radio transmitters. The inset shows a spectrum recorded at Tromsø for an HF heater frequency of 4.04 MHz. Otherwise the scales are identical to those in the Arecibo spectrum. After *Thidé et al.*[32]

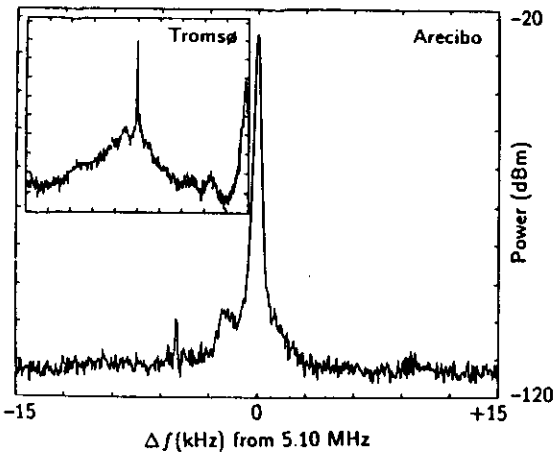

Figure 13. Same as Fig. 12 except for the Arecibo HF frequency (5.10 MHz) and that now the broad downshifted feature is almost totally absent while there is a strong, narrow SEE peak at −2 kHz. Interfering signals are present at −5 kHz. The inserted Tromsø spectrum, containing a SEE peak also at about −2 kHz show additional SEE features absent in the Arecibo spectrum. Presumably, this is in part due to the higher effective noise floor in Arecibo. After *Thidé et al.*[32]

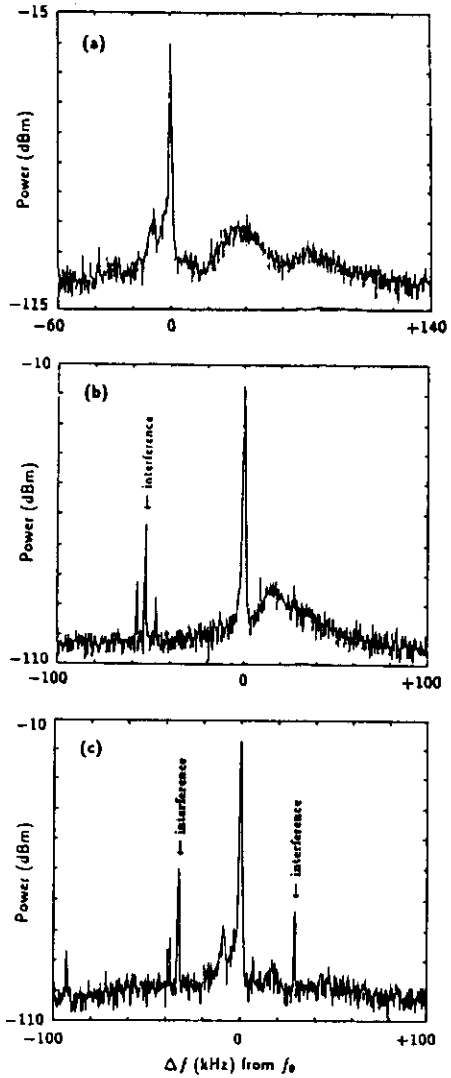

Figure 14. Spectra of stimulated EM emission at Tromsø for pump frequencies f_0 = 5.443 MHz (a), 5.403 MHz (b), and 5.383 MHz (c). The spectra were recorded at Tromsø on 12 May, 1988. The narrow features at ≈ −47, −53, and −57 kHz relative to f_0 in (b), and the corresponding features in (c) are interferences from nearby HF transmitters.

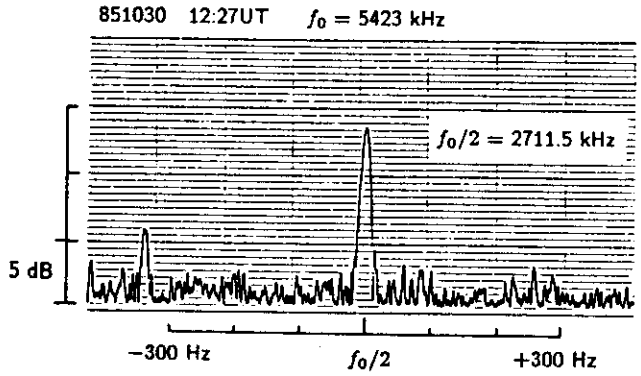

Figure 15. The spectrum of the stimulated emission at the heater subharmonic $f_0/2 = 5423/2 = 2711.5$ kHz. The observation was made during Tromsø heating experiments. After *Derblom et al.*[36]

length. The TPD may be an alternative, but the absence of any signatures whatsoever on $3\omega_0/2$ seems to indicate that TPD is not the prime candidate.[36]

Also, harmonics of the pump frequency may be excited in the ionosphere. The three spectra in Fig. 16 around $2\omega_0$ were obtained within 4 mins on the evening of October 26, 1984; the two top ones have been averaged in order to enhance the systematic features. Note the substantial variability in shape of the spectra with time, a fact which in itself can be taken as evidence of a natural phenomenon and not a weak scattering of the second harmonic from the transmitter. This is supported by the top panel spectrum in which only the sidebands around the exact second harmonic, but not the harmonic itself, are observed. The sideband features have been interpreted in terms of a four wave process involving three photons and an ion cyclotron mode and therefore this technique may be used to determine, at least approximately, the ion mass if the magnitude of the geomagnetic field is known or *vice versa*.[36]

7. Summary

In a large number of experiments carried out for almost twenty years at different ionospheric modification facilities, the near-Earth plasma has been subjected to strong HF radio wave irradiation and its response has been measured in various ways. Often, the results are in sharp disagreement with linear theory. Instead, nonlinear phenomena are excited and the experiments continue to shed new light on nonlinear wave–wave interactions and related phenomena. With the powerful space physics facilities at our disposal we can use the ionosphere as a giant laboratory for testing the fundamentals of modern plasma physics. In the true vein of this type of research, the experiments have clearly demonstrated that there is a wealth of the physics that is poorly understood and it is therefore important that this type of research be pursued with improved and refined methods. Such work will be

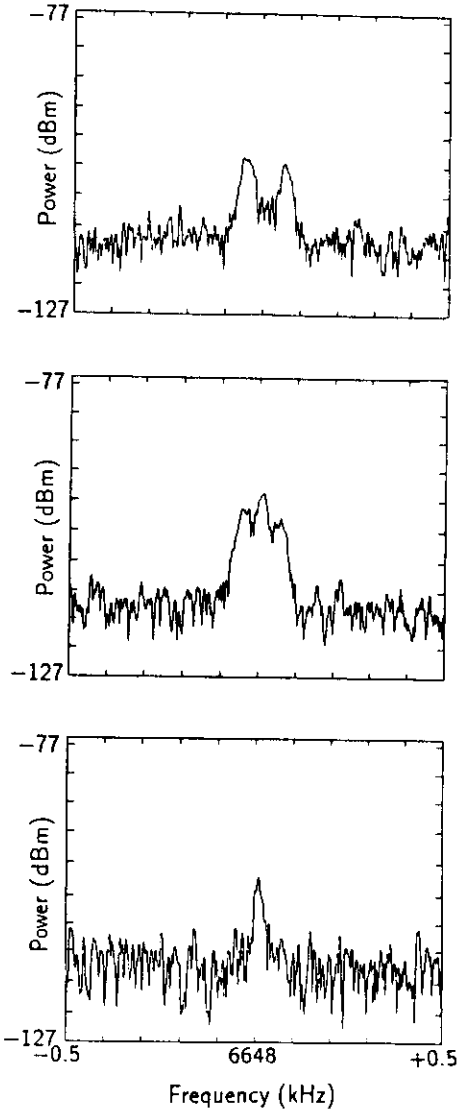

Figure 16. Second harmonic spectra obtained near Tromsø showing a considerable variability with time. Heater frequency $f_0 = \omega_0/(2\pi) = 3324$ kHz. After *Derblom et al.*[36]

beneficial not only for space plasma physics but for plasma physics as a whole.

Whereas there was a rather good agreement between parametric theory and early observations, mainly with incoherent scatter radars, later experiments, as some of those presented here, have clearly shown that better theories are required in order to explain all phenomena observed. So, the explanation of the physics of ionospheric modification still constitutes a challenging plasma physical problem. Significant progress has been made in explaining, at least partly, specific observations in terms of parametric instabilities and various propagation and conversion mechanisms. However, even for these specific problems the theory is often too simplistic.

For instance, it has been possible to explain SEE in terms of parametric interactions, but it is required that linear mode conversion takes place, both from electrostatic waves to electromagnetic waves and from the electromagnetic pump wave to electrostatic waves. It is therefore important to investigate the mode conversion processes in detail.

Also, the effects of plasma density gradients and external magnetic fields on the nonlinear interaction between the waves and the generation of electromagnetic radiation should be studied self-consistently. This pertains both to Langmuir and ion-acoustic waves in plasma density cavities due to the standing pump wave or Langmuir cavitons as well as upper hybrid and lower hybrid waves in geomagnetic field-aligned striations. Caviton formation can be explained within strong turbulence theory and it therefore seems natural to expand this theory to include effects and conditions which are important in space plasmas.

Acknowledgments. Parts of these notes are based on material presented by Dr. Thomas Leyser in his doctoral dissertation.[34] The author gratefully acknowledges a grant from the Swedish Natural Science Research Council (NFR) and the logistic support from the Arecibo Observatory, Puerto Rico, and the Auroral Observatory, Tromsø, Norway.

The Heating project has been financially supported by the Deutsche Forschungsgemeinschaft. The Arecibo Observatory is part of the National Astronomy and Ionosphere Center and is operated by Cornell University under contract with the National Science Foundation.

References

[1] Tellegen, B. D. H., Interaction between radio waves, *Nature, 131*, 840 (1933).

[2] Carlson, H. C., Jr., and L. M. Duncan, HF excited instabilities in space plasmas, *Radio Sci., 12*, 1001–1013 (1977).

[3] Stubbe, P., *et al.*, Ionospheric modification experiments in northern Scandinavia, *J. Atmos. Terr. Phys, 44*, 1025–1041 (1982).

[4] Stubbe, P., and H. Kopka, Summary of results obtained with the Tromsø heating facility, *Radio Sci., 18*, 831–834 (1983).

[5] Djuth, F. T., HF-induced radar backscatter, *J. Atmos. Terr. Phys., 47*, 1225–1243 (1985).

[6] Duncan, L. M., The HF-induced plasma line, electron acceleration, and resulting airglow, *J. Atmos. Terr. Phys., 47*, 1267–1281 (1985).

[7] Stubbe, P., *et al.*, Ionospheric modification experiments with the Tromsø Heating Facility, *J. Atmos. Terr. Phys., 47*, 1151–1163 (1985).

[8] Thidé, B., Parametric and related nonlinear wave–wave interactions in the ionosphere, *J. Atmos. Terr. Phys., 47*, 1257–1265 (1985).

[9] Erukhimov, L. M., S. A. Metelev, E. N. Myasnikov, N. A. Mityakov, and V. L. Frolov, Artificial ionospheric turbulence, *Radiophys. Quantum Electron., 30*, 208–225 (1987).

[10] Thidé, B., H. Kopka, and P. Stubbe, Observations of stimulated scattering of a strong high-frequency radio wave in the ionosphere, *Phys. Rev. Lett., 49*, 1561–1564 (1982).

[11] Lundborg, B., and B. Thidé, Standing wave pattern of HF radio waves in the ionospheric reflection region, 1, General formulas, *Radio Sci., 20*, 947–958 (1985).

[12] Lundborg, B., and B. Thidé, Standing wave pattern of HF radio waves in the ionospheric reflection region, 2, Applications, *Radio Sci., 21*, 486–500 (1986).

[13] Thidé, B., and B. Lundborg, Structure of HF pump in ionospheric modification experiments. Linear treatment, *Phys. Scr., 33*, 475–479 (1986).

[14] Budden, K. G., *The propagation of radio waves*, Cambridge University Press (1985).

[15] Abramowitz, M., and I. E. Stegun, *Handbook of Mathematical Functions*, 10th ed., National Bureau of Standards, United States Department of Commerce, Washington, D. C., p. 478 (1972).

[16] Gurevich, A. V., *Nonlinear Phenomena in the Ionosphere*, Springer-Verlag, New York (1978).

[17] DuBois, D. F., and M. V. Goldman, Radiation-induced instability of electron plasma oscillations, *Phys. Rev. Lett., 14*, 544–546 (1965).

[18] Silin, V. P., Parametric resonance in plasma, *Sov. Phys. JETP, 21*, 1127–1134 (1965).

[19] Nishikawa, K., Parametric excitation of coupled waves. I. General formulation, *J. Phys. Soc. Japan, 24*, 916–922 (1968).

[20] Nishikawa, K., Parametric excitation of coupled waves. II. Parametric plasmon-photon interaction, *J. Phys. Soc. Japan, 24*, 1152–1158 (1968).

[21] Perkins, F. W., C. Oberman, and E. J. Valeo, Parametric instabilities and ionospheric modification, *J. Geophys. Res., 79*, 1478–1496 (1974).

[22] Fejer, J. A., Ionospheric modification and parametric instabilities, *Rev. Geophys., 17*, 135–153 (1979).

[23] Tsytovich, V. N., *Nonlinear effects in plasma*, Plenum Press, chap. V (1970).

[24] Carlson, H. C., W. E. Gordon, and R. L. Showen, High frequency induced enhancements of the incoherent scatter spectrum at Arecibo, *J. Geophys. Res., 77*, 1242–1250 (1972).

[25] Wong, A. Y., and R. J. Taylor, Parametric excitation in the ionosphere, *Phys. Rev. Lett., 58*, 1375–1378 (1987).

[26] Showen, R. L., and D. M. Kim, Time variations of HF-induced plasma waves, *J. Geophys. Res, 83*, 623–628 (1978).

[27] Birkmayer, W., T. Hagfors, and W. Kofman, Small-scale plasma-density depletions in Arecibo high-frequency modification experiments, *Phys. Rev. Lett.*, *57*, 1008–1011 (1986).

[28] Nordling, J. A., Å. Hedberg, G. Wannberg, T. B. Leyser, H. Derblom, H. J. Opgenoorth, H. Kopka, H. Kohl, P. Stubbe, M. T. Rietveld, and C. LaHoz, Simultaneous bistatic European Incoherent Scatter UHF, 145-MHz radar and stimulated electromagnetic emission observations during HF ionospheric modification, *Radio Sci*, *23*, 809–819 (1988).

[29] Nordling, J. A., Ionospheric parameters derived from heater enhanced plasma lines, *J. Geophys. Res.*, in press (1989).

[30] Isham, B., W. Kofman, T. Hagfors, J. Nordling, B. Thidé, C. LaHoz, and P. Stubbe, New phenomena observed by EISCAT during RF ionospheric modification experiments, submitted to *Radio Sci.* (1989).

[31] DuBois, D. F., H. A. Rose, and D. Russell, Excitation of strong Langmuir turbulence in HF heating of the ionosphere: cavitons vs. parametric instabilities, Los Alamos Preprint (1988).

[32] Thidé, B., Å. Hedberg, J. A. Fejer, and M. Sulzer, First observations of stimulated electromagnetic emission at Arecibo, *Geophys. Res. Lett.*, in press (1989).

[33] Stubbe, P., H. Kopka, B. Thidé, and H. Derblom, Stimulated electromagnetic emission: A new technique to study the parametric decay instability in the ionosphere, *J. Geophys. Res.*, *89*, 7523–7536 (1984).

[34] Leyser, T. B., Stimulated electromagnetic emission in the ionosphere, Doctoral dissertation at Uppsala University, *IRF Scientific Report*, 198 (1989).

[35] Leyser, T. B. and B. Thidé, Effect of Pump-Induced Density Depletions on the Spectrum of Stimulated Electromagnetic Emissions, *J. Geophys. Res.*, 93, 8681–8688 (1988).

[36] Derblom, H., B. Thidé, T. B. Leyser, J. A. Nordling, Å. Hedberg, P. Stubbe, H. Kopka, and M. Rietveld, Tromsø heating experiments: stimulated emission at HF pump harmonic and subharmonic frequencies, *J. Geophys. Res*, in press (1989).